



GEOPHYSICAL METHODS APPLIED TO THE ASSESSMENT OF THE GEOLOGICAL AND GEOTECHNICAL CONDITIONS OF DAM SITES: THE CASE STUDY OF PEDRÓGÃO DAM (PORTUGAL)

Rogério Mota^{*}, Jorge Neves[†], and Fernando A. Monteiro dos Santos[‡]

^{*} Laboratório Nacional de Engenharia Civil (LNEC)
Av. do Brasil, 101, 1700-066 Lisboa, Portugal
e-mail: rmota@lnec.pt

Keywords: Dams, Geophysical methods, Foundation; Geological-geotechnical data; Porosity section; Water content section.

Abstract. *Geophysical methods are indirect tools of investigation of the subsoil. Seldom is the geophysicist able to confirm the results of his models with the reality. In the case study of Pedrógão dam, this was possible. At this site several geophysical methods were applied and compared with the geological and geotechnical map of the excavations for the dam's foundation. This analysis allowed the conclusion of a good match between the main geophysical anomalies of each physical parameter with the identified main geological structures, namely an important fault zone – that could be a seepage source -, and also a good fit of the predicted in depth development of the geotechnical zones.*

1 INTRODUCTION

LNEC has a long experience in the use of geophysical surveys to assess the geological and geotechnical condition of dam sites. The cooperation between LNEC and EDP is as long as more than half a century, with surveys performed in Portugal and African countries using mainly resistivity maps and seismic refraction profiles for dam site studies. In the case study of Pedrógão Dam, seismic tomographic sections were performed between the geological survey's boreholes and between these boreholes and the surface, along with seismic refraction profiles and measurements of resistivity along lines using the Schlumberger array with two depths of investigation^{1,2}. Later, in the aim of an academic work³ a self-potential map and resistivity profiles were performed at the right river bank in the same location of the refraction ones.

Geophysical models produced with some of the collected data were compared with the geological and geotechnical data gathered during the design phase surveys and especially with the one obtained through the geological and geotechnical mapping of the excavations for the dam's foundation.

Refraction and resistivity data were jointly processed in order to produce sections of porosity and water content⁴.

Comparative analysis of geophysical models and geological-geotechnical data from the excavated dam foundation surface present a good match between the main geophysical

[†]EDP - Gestão da Produção de Energia, S.A. (e-mail: jorgepacheco.neves@edp.pt)

[‡]Faculdade de Ciências da Universidade de Lisboa (e-mail: fasantos@fc.ul.pt)

anomalies and the identified main geological structures, namely an important fault zone, but also with the predicted in depth development of the geotechnical zones.

Geotechnical sections of porosity and water content and the excavated rock mass have also a good match.

2 MATERIALS AND METHODS

2.1 Study site

The study site here presented is one of the locations surveyed for the implementation of Pedrógão Dam (Figure 1). This dam is integrated in the Alqueva multi-purpose development and provides water for irrigation and the flow modulation from Alqueva Dam, as well as the production of electricity. It is the first dam built in Portugal with Roller Compacted Concrete (RCC).

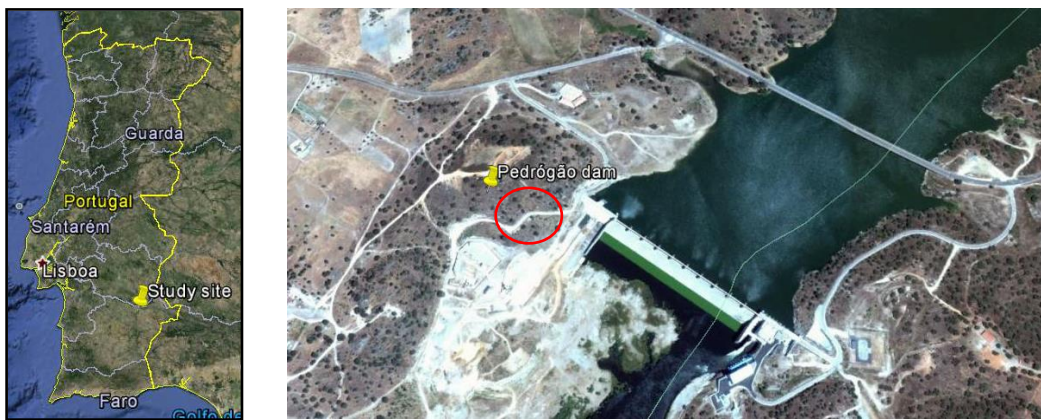


Figure 1: Site location within Portugal and study area (red circle) on the aerial photograph (Google Earth).

2.2 Geological setting

The Pedrógão Dam is located in a wide meander of the Guadiana River, on a two mica, medium to fine grained, porphyritic rock mass corresponding to a roughly triangular outcrop of the middle Carboniferous granitic batholith that intruded the pre-existent metasedimentary and metavolcanic Ordovician to Silurian aged rocks.

At the right bank of the dam site, between elevations 80 and 66, occurs a river terrace of the late Pleistocene, largely eroded, that consists of sand and silt with rolled stones mostly of quartz and quartzite, covered with sparse granitic blocks of colluvium nature. At the surface, this terrace had an inclination of approximately 12° with the horizontal. Between elevations 66 and 60, the terrace slope was almost horizontal (3°), with river eroded moderately weathered granitic outcrops and partly covered by alluvium.

The possibility of the presence of a large sub-vertical fault marked in the 1:50000 scale sheet 43-B⁵ of the geological map of Portugal was considered and investigated.

In a geological section⁶ by the planned dam axis (Figure 2) is synthesized the relevant information obtained from geological and geotechnical exploration works carried out during the dam design phase. It shows the boreholes used for subsurface geological exploration, permeability tests and geotechnical characterization, where several seismic tomography profiles were obtained, showing also the limits of both refraction and resistivity profiles.

In this section, numerous structures are indicated - faults, fault zones and fracture alignments – that can be distinguished by the greater length and the smaller thickness of the faults/fault zones whose filling consists of clay and crushed/very fractured granite and/or

breccia, while the fracture alignments are formed by closely spaced joints, normally filled with millimetre thick clay, separated by moderate (W3) to highly weathered (W4) granite.

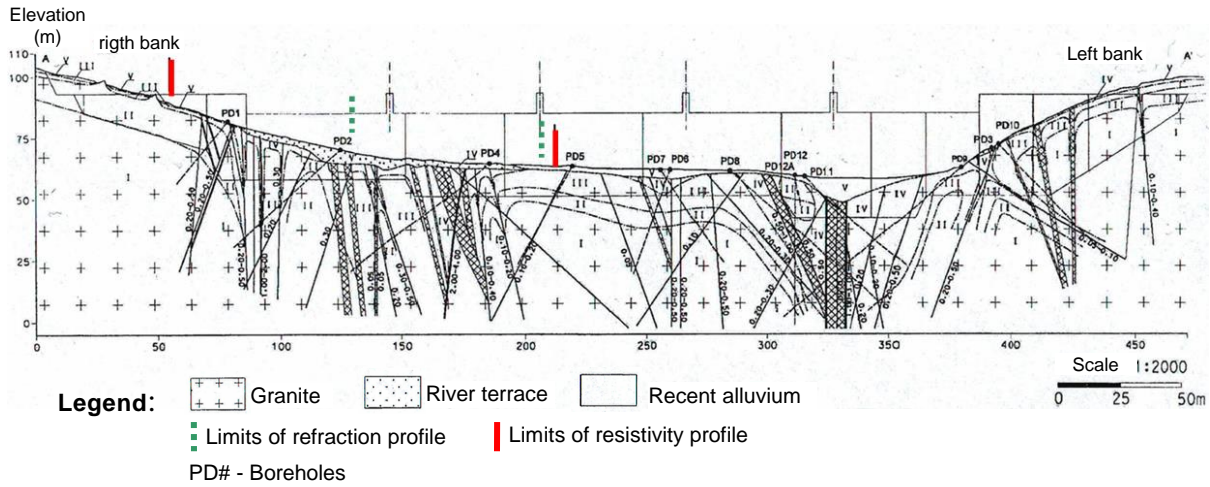


Figure 2: Geological-geotechnical section through the dam axis (adapted from Neves et al.⁶)

The weathering grade (W) and the fracturing spacing (F) classification of the rock mass, used in geological and geotechnical zoning shown in Figure 3, is summarized in Table 1, following the ISRM⁷ criteria. Analysis of borehole cores and geological mapping gave weathering and fracturing results, while V_p was obtained from seismic tomography.

ZG3B	W4-W5	F4-F5	$V_p < 2500$ m/s
ZG3A	W3-W4, rarely W5	F3-F5	
ZG2	W3, rarely W2 or W4	F3-F4, rarely F5	$2500 < V_p < 4000$ m/s
ZG1	W1-W2, rarely W3	F2-F3, rarely F4 or F5	$V_p > 4000$ m/s

Table1: Geotechnical zones general characterization (adapted from Neves⁸).

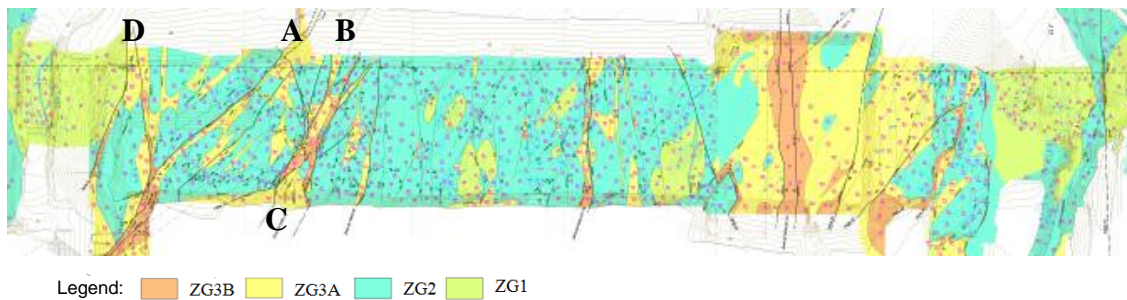


Figure 3: Geological and geotechnical map (out of scale) of the excavated dam foundation surface⁸, with the identification of geotechnical zones (ZG). A to D – Faults zones, crossed by the geophysical profiles.

ZG3B and ZG3A zones (Figure 3) have a poor to very poor geomechanical quality, high weathering grade (W3 to W5) and close fracture spacing (F3 to F5). They constitute the most superficial part of the rock mass, the fault zones and its vicinity, as well as the rock material present within a considerable part of the fracture alignments. ZG2 is a rock mass of fair to good geomechanical quality, characterized by intermediate weathering grade and fracturing spacing (W2 to W3, F3 to F4 and, occasionally, F2 or F5). ZG1 is a rock mass of good to very good geomechanical quality (W1 to W2, F2 to F3 and, rarely, F4 or F5).

Figure 4 illustrates some of the faults at the right bank, identified by the letters A and C in Figure 3 that were intersected by the geophysical exploration works. According to Neves⁸, the rock mass between these two points was highly fractured and had a reddish colour due to the

presence of abundant iron oxides, indicating intense water percolation. The fault zone identified with **B** and **C** includes clay filled faults and a 10 m thick heterogeneous zone (right picture on Figure 4), filled with a clayey material with very weak geomechanical characteristics, that implied the excavation and concreting of an upstream-downstream 3 m high trench across the dam foundation, below the previewed excavation level.

At **D** (Figure 3), there is a sharp transition, intersected by PD1 borehole, between the poor to fair quality rock mass belonging to ZG3 and ZG2, and the good to very good quality rock mass from ZG1. At the contact between these two geotechnical zones, there is a fault filled with clay and crushed rock with thickness up to 0.5 m, sometimes associated with highly weathered granite (W4-W5), with a total thickness of about 2 m.



Figure 4: Fault zones crossed by the geophysical profiles. *Left* - zone **A** on Figure 3. *Right* - the downstream limit (point **C**) of the fault zone **B-C** on Figure 3⁸.

2.3 Geophysical surveys

Figure 5 illustrates the position of most of the surveys, and their relative positions to the dam axis, which is centered on the excavated surface presented in Figures 3 and 4.

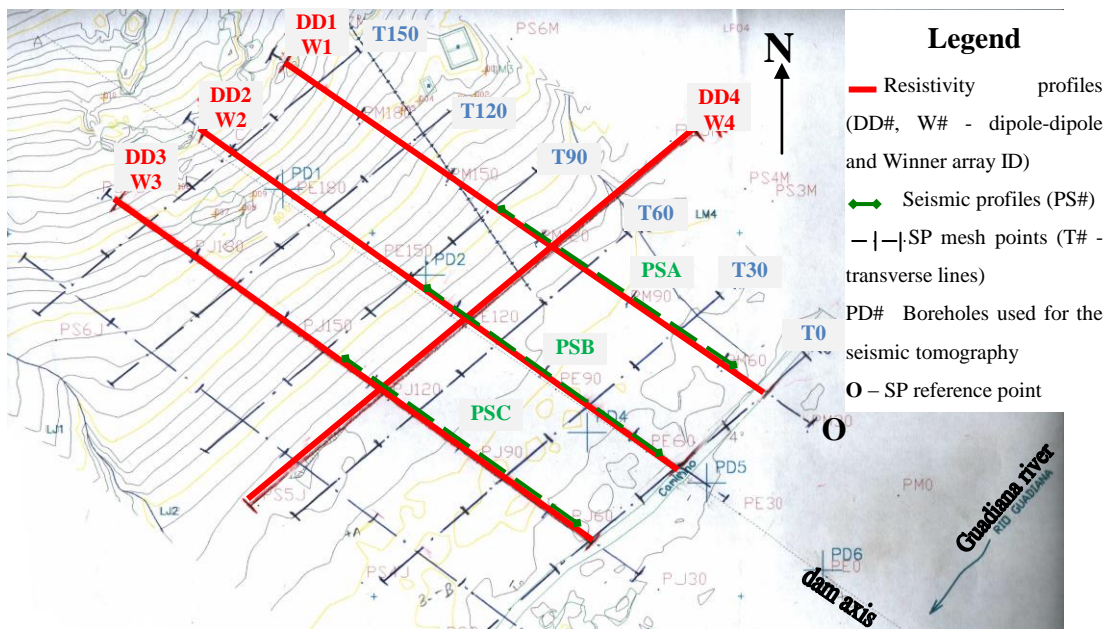


Figure 5: Location of most of the geophysical surveys performed at the site.

2.3.1 Borehole seismic tomography

Borehole seismic tomography involves a large number of raypaths between boreholes (cross-hole tomography) and/or between them and the surface (Figure 6). It's a method

applied with success to assess rock massif, and it is being applied in Portugal in the past 25 years mainly to assess the treatment of dam foundations.

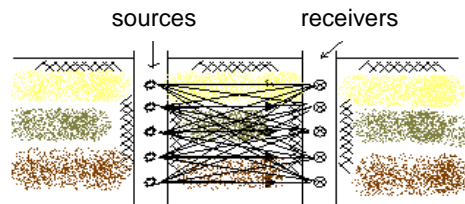


Figure 6: Scheme of data acquisition. Seismic wave generated at each shot is recorded in all the receivers.

Usually the boreholes are vertical, which wasn't the case in here since they were bored for the geological survey, and it was necessary to cross geological structures inferred from the surface. Due to this reason, the seismic tomographic profile through the dam axis was obtained by projecting the holes in a virtual vertical plane passing through their tops.

Twelve holes were used between both river banks. Seismic tests were performed between holes and between holes and the surface, which enabled to achieve 5 seismic profiles between holes (one across the river) and 6 seismic fans between holes and the surface². A part of the profile carried out between both river banks, situated in the right bank (between holes PD1 and PD4), was used to compare with the other methods performed in the same location.

The results were processed with a software package developed by Pessoa⁹ based on the iterative inversion method SIRT (Simultaneous Iterative Reconstruction Technique) considering straight paths for seismic rays. Instant electric detonators were used each 3 m as seismic source and the hydrophone string had receivers spaced by 3 m.

2.3.2 Refraction

Of the ten seismic refraction profiles made in the right river bank to the dam project phase¹, seven were oriented roughly parallel to the river and three normal to it. The latter have now been reprocessed with Rayfract® program. The central one was approximately coincident with the axis of the dam (Figure 5) and the two others were located 30 m upstream and downstream of it. Each profile was performed with 24 geophones spaced 3 m, and 14 shots - two of them out to the geophones line - with a total length of 75 m.

2.3.3 Electrical Resistivity Tomography (ERT)

ERT (dc method) is a geophysical imaging technique used to generate 2D/3D models, or images, of the subsurface resistivity distribution. Data collection and processing methodologies are widely described in the literature¹⁰, and so only a brief description is provided here. ERT surveys involve making a large number of four-point direct current (DC) electrical measurements (pairs of current and potential electrodes) using computer controlled automated measurement systems and multi-electrode arrays. These data are inverted with Res2DInv¹¹ to produce images of the subsurface.

Eight profiles were performed on four alignments; three of them normal to the river and coincident with the seismic refraction profiles and the fourth one parallel to the river (see Figure 5). In each alignment both dipole-dipole and Wenner array were used.

The profiles were performed with 4 m of dipole distance, for a total length of 160 m.

2.3.4 Self-potential (SP)

SP method can be an important complement to the dc method in near-surface groundwater flow detection¹², since it is based on measurements of the steady state natural electrical

potentials existing on the ground surface. As SP electrodes measures the difference in redox potential (geochemical oxidation-reduction reactions) between the reference electrode and the roving one, SP anomalies are due to current flow between different environments and so it can give an indication of the presence of water flow through rock fractures. SP measurements were performed according to the mesh shown on Figure 5, with the front electrode alternating with the rear one to cancel electrodes polarization. Measurement distance was 30 m, and point O in Figure 5 is regarded as the reference (zero potential).

2.3.5 Porosity and water content 2D sections

Electrical resistivity is a volumetric property, sensitive to water mineralization and content, and also to porosity and clay. Seismic velocity is also a volumetric property, which is sensitive, among others, to porosity. So the combined use of both physical properties of soils and rocks can allow estimating its porosity. Mota^{3,4} developed a software (RSAnn) that can produce 2D sections of porosity and of water content using a stochastic approach to combine resistivity and seismic refraction models.

3 RESULTS AND DISCUSSION

3.1 Borehole seismic tomography

Of the various seismic tomography profiles performed, a sample from the one that runs between the two river banks, and corresponding to the zone of the right bank where the other geophysical methods were used, is presented in Figure 7, as well as an extract from the profile performed between PD1 and the surface.

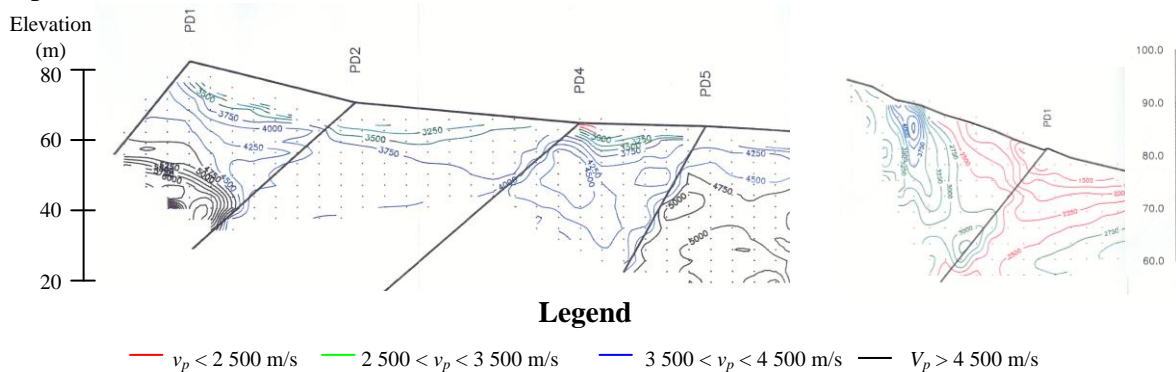


Figure 7: **Left** - Extract from the seismic tomography profile obtained between the two banks of the Guadiana river². **Right** - Extract from the tomography performed between the borehole PD1 and the soil surface².

The tomography between the two river banks reveals that between boreholes PD2 and PD4 v_p is generally below 4000 m/s, and its highest values (> 5000 m/s) occur in depth below the top of PD1 and between boreholes PD5 and PD6. The latter is outside the area surveyed by the other methods. The leaning of PD1 into the mass of good mechanical quality influenced the outcome of this tomography, which was unable to pinpoint the fault zone **D**. However, due to the influence of the weathered and fractured surface layer, the tomography obtained between the hole and the surface highlights this geological feature. In the event that only this method was used these results would be contradictory, which highlights the need to conduct a geophysical survey with different methods.

3.2 Seismic refraction

The seismic refraction profiles reprocessed with Rayfract® led to the models shown in

Figure 8. These models are aligned such that a straight line through all defines a line perpendicular to the axis of the dam.

The velocity field varies from less than 500 m/s in the top layers and at high topographic levels to more than 4500 m/s in depth.

The analysis of the models allows the following conclusions:

- identification of the fault zone marked by **B** and **C** on Figure 3, characterized by a depression in the 3000 m/s contour line, with a good fit with the mapped direction;
- good fit of the width (10 m) of the low v_p anomaly in the downstream profile, with the size of the **B-C** fault zone on site **C** (right photo on Figure 4);
- the thickness of the top layer, characterized by velocity below 2500 m/s and above approximately elevation 60 m, increases as the topography increases - which is more evident in the central and downstream profiles.

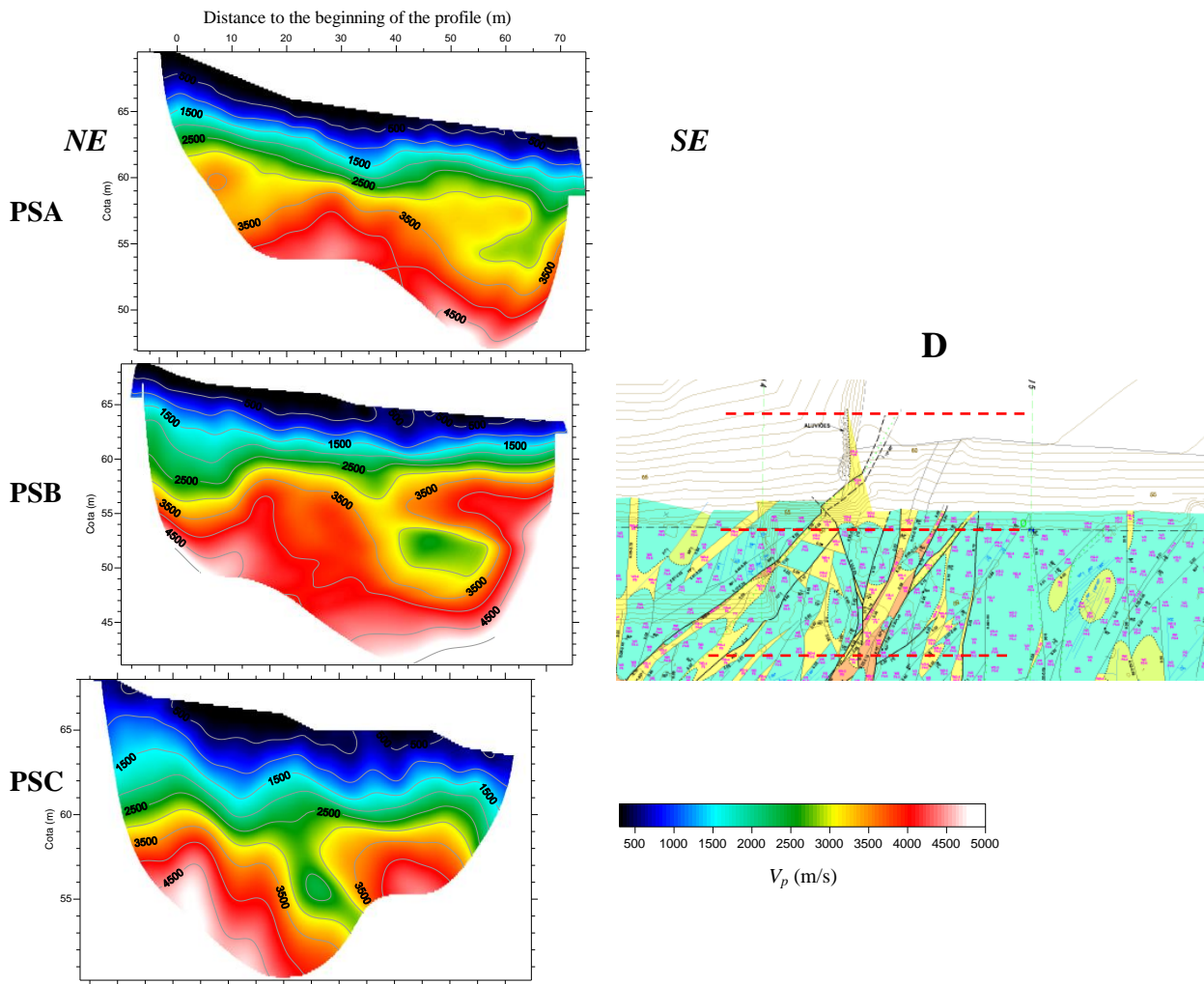


Figure 8: Seismic refraction models: **PSA** to **PSC** – upstream; central and downstream profiles; **D** - approximate location of profiles (red lines), in the extract of the geological and geotechnical map⁸.

3.3 Electrical Resistivity Tomography (ERT)

ERT models obtained for both arrays were similar. So, since resistivity lateral variations were the main goal of this method, due to the orientation of the profiles versus the dominant geologic structures, and the dipole-dipole array is the best one for this purpose, only the models obtained with this array are presented in Figure 9. The models are characterized in general by relatively low values of resistivity: 40-1000 ohm.m. The

relative E-W positioning of the parallel profiles reflects its positioning in the field so that a straight vertical line through all models defines a line perpendicular to the dam axis.

Positions of the boreholes used to perform the seismic tomography profile are indicated in the central profile model (axis of the dam). On this model **B** and **D** correspond to the fault zones marked in the same way on Figure 3, and illustrated with photos in Figure 4, showing a good fit between the location and size of low resistivity anomalies and the faults identified in the field.

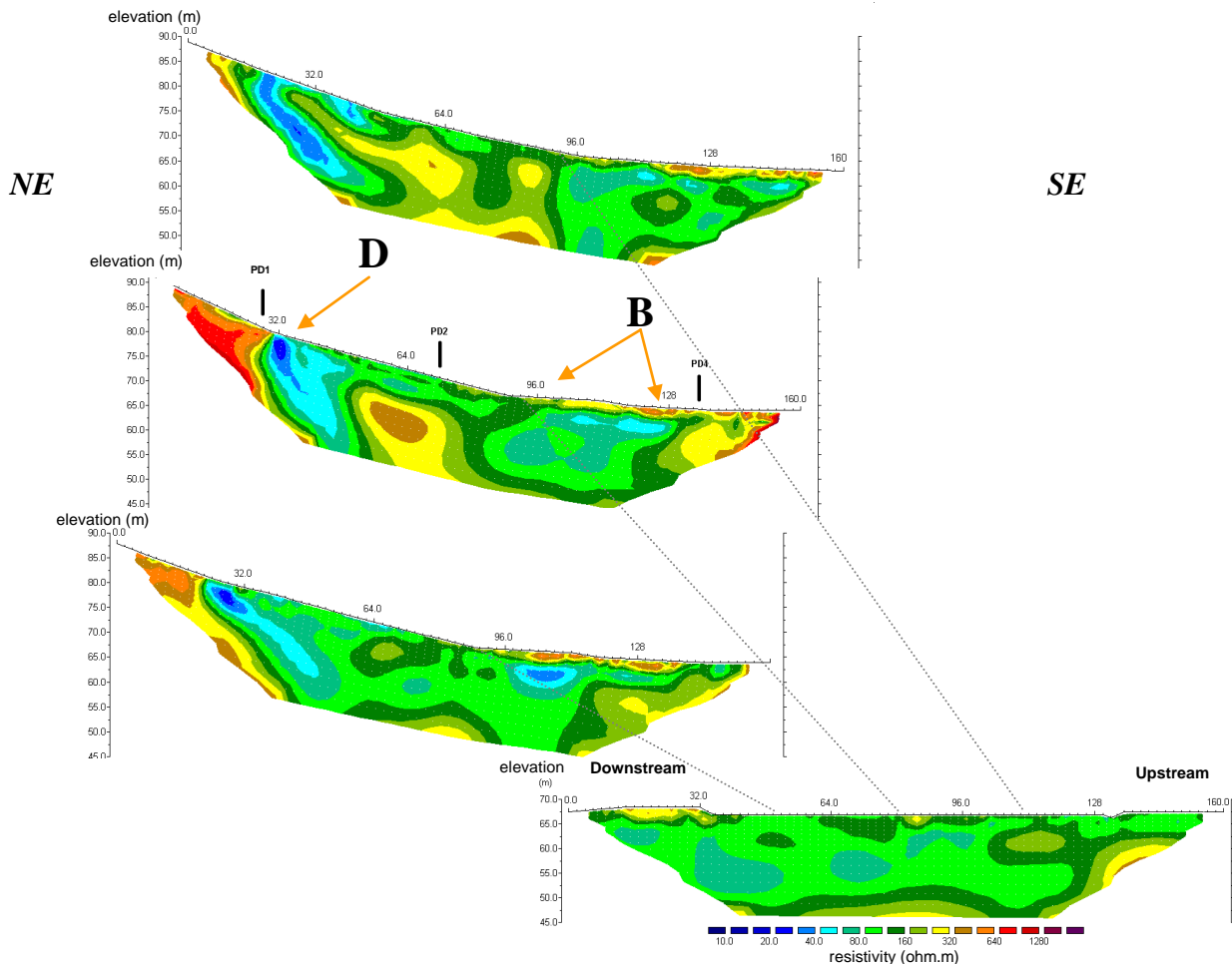


Figure 9: Resistivity models: *from top to bottom*: upstream; central; downstream and profile normal to these. **D** and **B** – Fault zones on Figure 3. Normal profile and parallel ones crossing positions are marked with dashed grey lines.

Low resistivity anomalies (<40 ohm.m) occur near borehole PD1 in the central profile and in identical positions in the upstream and downstream profiles, and also at lower elevations (closer to the river) in all of these profiles at distances above 100 m which have a good correspondence in the normal profile.

The higher resistivity values occur at elevations above PD1 in the central profile and at the NW ends of upstream and downstream profiles. High values are also present at the SE end of the central profile, which corresponds to a location where the rock outcrops. These regions have a good fit with the best quality geomechanical areas.

There is also a good connection between the thicknesses of the river terrace, identified with borehole PD2, and the material with resistivity below 160 ohm.m, at the same place.

The combination of iron oxides, caused by the percolation of water in the various faults, with the presence of clay that fills them, are favourable to the conduction of electric current, which is evidenced by the low values of electrical resistivity obtained. A

geological environment characterized by a granite substrate without faults has high values of the electrical resistivity, which doesn't happen at this site, doe confirming the presence of faults.

3.4 Self-potential (SP)

The SP map produced is presented in Figure 10. Coordinates are considered with respect to the reference point. Since topography is one of the factors that influence SP, this was integrated in the SP map, and the result is presented in the same figure. The analysis of these results shows that the minimum are aligned with the fault zone **B** (Figure 3), so this minimum is associated with the water flowing on it.

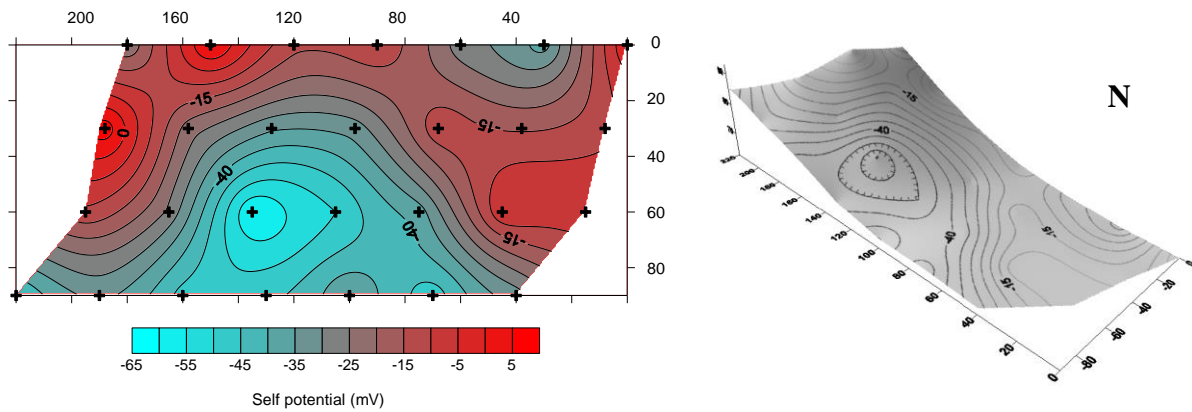


Figure 10: Self-potential map. *Left* – without topography. *Right* – with topography.

3.5 Porosity and water content 2D sections

Taking the coincident implementation of seismic refraction and electrical resistivity profiles a joint processing of the models obtained along the axis of the dam was made with RSAnn software⁴. The resulting sections of porosity and water content are presented in Figure 11. From the analysis of the results obtained it highlights the overlapping of the area with the largest water content and higher porosity and the mapped region with the same size crossed by several faults and worst geomechanical characteristics.

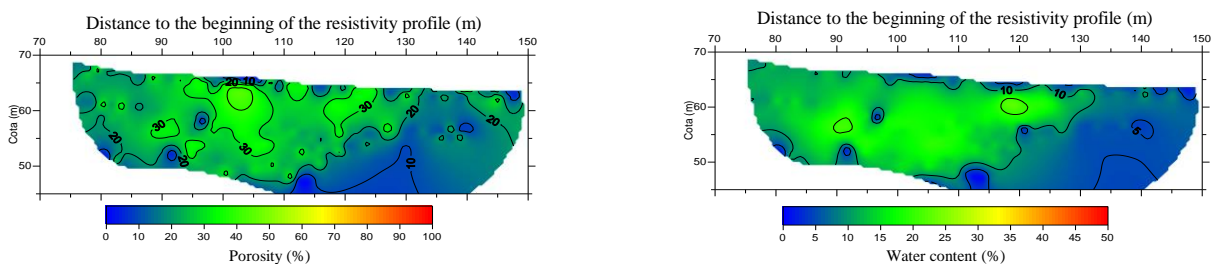


Figure 11: Sections produced with RSAnn software⁴ from the central models of resistivity and porosity. *Left* - Porosity section. *Right* – Water content.

For a better comparison of the results obtained with the various geophysical methods, Figure 12 depicts models obtained in the dam axis with ERT, seismic refraction and seismic cross-hole tomography methods, as well as the geological and geotechnical map of the dam foundation after excavation of its granite massif. Contours of SP map are superimposed on the latter. For ease of interpretation, all results are presented on the same scale. Two red dotted lines overlapping the resistivity model identify the elevation of the mapped excavated foundation. The analysis of this figure allows noting the good agreement of the geological and

geotechnical mapping performed after excavation of the dam foundations with the results obtained from the various geophysical methods.

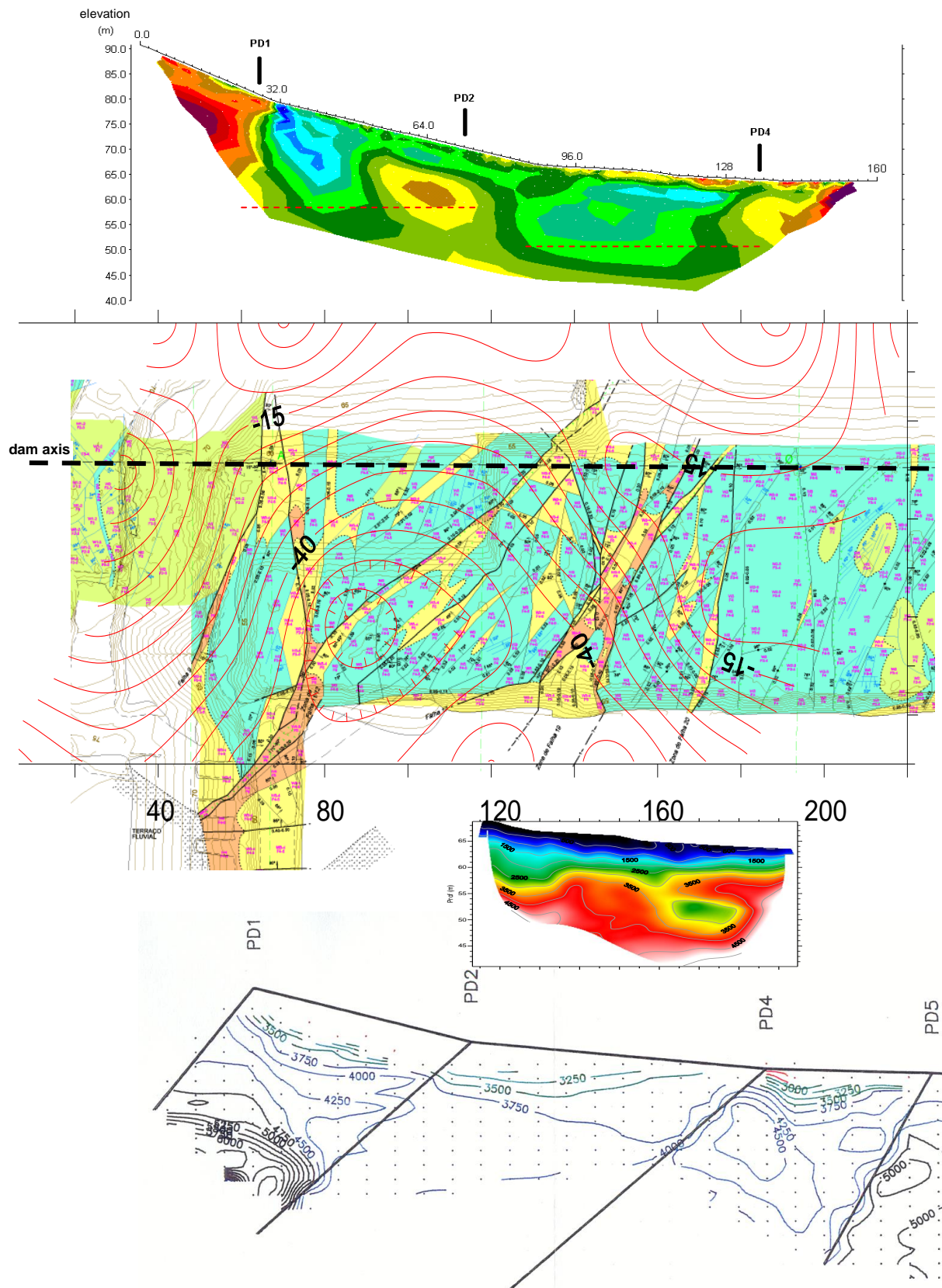


Figure 12: **A** – Resistivity central model. **B** - Extract of the geological and geotechnical map⁸, with superposition of isolines of the SP map. **C** – Seismic refraction central model. **D** – Extract of the seismic tomographic profile².

4 CONCLUSIONS

The comparison between the results obtained by indirect - geophysical - and those by direct means - geological and geotechnical mapping of the excavated mass - has clearly validate the origin of the anomalies identified with each geophysical method, allowing thus to overcome the ambiguity associated with the interpretation of the models resulting from data collected by different geophysical methods.

The results of this study allow highlighting the advantages of borehole seismic tomography in the study of dam sites, namely:

- investigation in depth, with high precision, depending on the spacing used in tests;
- filtering the influence of topsoil;
- achievement of a 2D section between the two river banks.

In a cost-benefit perspective, it turned out that, if the target was only the study of the top 20 m of land on the river bank, seismic refraction and electrical resistivity would be more economic and achieving conclusive results in a small fraction of the time compared to cross-hole seismic tomography, which involves, in addition to carrying out the tests, already more time-consuming, the highly expensive implementation of the boreholes, if it wasn't the case that they must be performed for the geological-geotechnical survey.

This work made possible to show that the use of more than one geophysical method reduces the ambiguity in the interpretation of geophysical anomalies present in the individual models.

An added value in the combined use of seismic refraction and electrical resistivity methods is that it allows obtaining estimates for geotechnical parameters that can help geotechnical classification of rock masses.

ACKNOWLEDGMENTS

We thank EDIA – Empresa de Desenvolvimento e Infra-estruturas do Alqueva, S.A., for the authorisation to use seismic tomography profile data and seismic refraction data collected during the project phase. We also thank EDIA and EDP – Gestão da Produção de Energia, S.A. for the authorisation for use and publication of geological and geotechnical data obtained and interpreted during the project and construction phases.

REFERENCES

- [1] R. Mota and L. Fialho Rodrigues, *Prospecção geofísica no local do Açude de Pedrogão*. Relatório 191/98, LNEC, Lisboa, Portugal (1998).
- [2] R. Mota and L.F. Rodrigues, *Prospecção geofísica complementar, por métodos sísmicos, no local de implantação do Açude de Pedrogão*. Relatório 260/99, LNEC, Lisboa, Portugal (1999).
- [3] R. Mota, *Methodologies of geophysical prospection applied to environmental and geotechnical problems. Joint use of electrical and seismic methods*, PhD thesis, Univ. Lisboa, Portugal (2006).
- [4] R. Mota and F.A. Monteiro Santos, *2D pseudo-sections of porosity and water saturation from combined resistivity and seismic surveys applied to hydrological and geotechnical studies*, Near Surface Geophysics, 2010, 8, pp 575-584, (2010).
- [5] A.B. Carvalhosa and A.M. Galopim de Carvalho, *Carta Geológica de Portugal. Escala 1/50000, Folha 43-B (Moura) e Notícia Explicativa*, Serv. Geol. de Portugal, (1970).
- [6] J. Neves, J.M. Cotelos Neiva and C. Lima, *Geologia e geotecnia do local da barragem de Pedrogão, no rio Guadiana*, VII Cong. Nac. Geotecnia, Porto, 263-272, (2000).

- [7] International Society for Rock Mechanics, Commission on Classification of Rocks and Rock Masses, *Basic Geotechnical Description of Rock Masses*, Int. J. Rock Mech. Min. Sci. & Geomech. Abstr., Pergamon Press Ltd, Vol. 18, pp.85 to 110, (1980).
- [8] J. Neves, *Escalão de Pedrogão - Cartografia Geológico-Geotécnica das Superfícies Escavadas*. Relatório P0962/04, EDP, Produção EM, SA., Porto, Portugal (2004).
- [9] M. Pessoa, *Aplicação de técnicas tomográficas à prospeção sísmica entre furos de sondagem*, Trabalho de síntese apresentado no âmbito das provas de aptidão pedagógica e capacidade científica na Universidade de Aveiro; Aveiro, Portugal (1990).
- [10] G.V. Keller and F.C. Frischknecht, 1966. *Electrical methods in geophysical prospecting*. Pergamon Press, (1966).
- [11] M.H. Loke and R.D. Barker, *Rapid least-squares inversion of apparent resistivity pseudosections by a quasi-Newton method*. Geophys. Prosp., 44: 131-152, (1996).
- [12] R. Mota, F.A. Monteiro Santos, A. Mateus, F.O. Marques, M.A. Gonçalves, J. Figueiras and H. Amaral, *Granite fracturing and incipient pollution beneath a recent landfill facility as detected by geoelectrical surveys*. J. Applied Geophysics 57, 11 –22, (2004).